Journal of Materials Chemistry C

PAPER

View Article Online
View Journal | View Issue

Cite this: J. Mater. Chem. C, 2019, 7, 3952

Stable soft cubic superstructure enabled by hydrogen-bond complex functionalized polymer/liquid crystal system†

Haiquan Li,[a] Wenbin Huang,[ab] Qinyu Mo,[a] Binghui Liu,[a] Dong Shen,[a] Weian Zhang *[a] and Zhi-gang Zheng *[ac]

Received 25th October 2018,
Accepted 21st February 2019

DOI: 10.1039/c8tc05390a

rsc.li/materials-c

A stable liquid crystal soft cubic superstructure (*i.e.*, blue phase) in a wide temperature range was achieved by photopolymerizing a judiciously designed hydrogen-bond (H-bond) complex functionalized polymer/liquid crystal system. Such an H-bond is generated through complexation between a polymerizable proton acceptor and a mesogenic proton donor, which plays a positive role in structural enhancement of a blue phase on one hand, and on the other hand enables the stabilization of such a cubic superstructure with a lower polymer content compared with that of conventional materials. Owing to the two aforementioned aspects, the driving voltage of such a system was reduced significantly, while a fast responsiveness of the blue phase (*i.e.*, submillisecond) was still maintained. A noteworthy aspect is that a weak electro-optical hysteresis of such blue phases, which is generally generated in a high polymer content system, has been achieved herein in a low polymer content system, due to the H-bond interaction between the mesogenic donor and the proton acceptor decorated polymer network. Herein, a stable blue phase II with a wide temperature range from 55.3 °C, spanning the whole room temperature range, to a temperature lower than −40 °C was obtained, and moreover its electro-optical performances at −15 °C were demonstrated. This work develops a new approach to stabilize a soft cubic superstructure with satisfying thermal and electro-optical performances, which may be a promising candidate or competitor with regards to conventional materials, thereby facilitating its practical applications in diverse perspective fields.

1. Introduction

Soft superstructures have a widespread and significant existence in nature, serving a variety of purposes. For instance, the helical organization of biopolymers in a beetle's exoskeleton makes it possible to exhibit spectacular iridescence under sunlight.[1] Inspired by the delicate, ingenious designs of nature, people have attempted to create and imitate novel soft superstructures[2] with advanced and intriguing functionalities for practical applications. Among these, blue phase liquid crystals (BPLCs) are attractive self-organized soft materials composed by double twisted aligned LC molecules (*i.e.*, double twisted cylinders, DTCs), exhibiting three sub-phases, BPIII,[3] BPII and BPI, as the sequence of temperature decreases. Early theoretical and experimental results have corroborated that BPII and BPI possess fantastic self-organized cubic superstructures, presenting simple cubic and body-centred cubic lattices, respectively, stacked by the DTCs separated by networks of disclination lines. BPLCs can serve a plethora of functions and are known to endow specific characteristics to materials,[4,5] paving ways for potential applications in new generation displays and versatile photonic devices.[6–8]

However, BPLCs only exist within a very narrow temperature range between the chiral nematic (N*) and isotropic phases, due to the requirement of a delicate balance between the free energy and topological confinement of such exotic systems.[9,10] This is an obstacle to practical applications, and thus several approaches,[5,11,12] such as loading nanoparticles,[13,14] doping bent-shaped molecules,[15,16] or even mesogen functionalized polymers[17,18] have been applied to widen their operating temperature ranges to cover the actual temperature range in daily life. The most universal, acceptable and commonly utilized methodology to broaden the BP range is polymer stabilization due to its outstanding effects to anchor the defect scaffolds. In such a polymer/liquid crystal system, the soft cubic superstructure was bound by photo-induced cross-linked polymer networks,

[a] Shanghai Key Laboratory of Functional Materials Chemistry, Department of Physics, East China University of Science and Technology, 130 Meilong Road, Shanghai 200237, China. E-mail: wazhang@ecust.edu.cn, zgzheng@ecust.edu.cn
[b] School of Optoelectronic Science and Engineering & Collaborative Innovation Center of Suzhou Nano Science and Technology, Soochow University, Suzhou 215006, China
[c] State Key Laboratory of Applied Optics, Changchun Institute of Optics, Fine Mechanics and Physics, Chinese Academy of Sciences, Changchun, 130033, China

† Electronic supplementary information (ESI) available. See DOI: 10.1039/c8tc05390a

forming the so-called polymer stabilized BPLC (PSBPLC), and thus resulting in a wide BP range over 60 °C.[15] PSBPLC has many intriguing properties such as a wide temperature range, a sub-millisecond response time, and excellent fatigue resistance.[19,20] In conventional PSBPLC systems, a significant amount of polymer networks (around 10 wt%[21,22]) is usually required to stabilize the BP structure over an appropriate and satisfying temperature range. However, a higher concentration of polymer networks usually degrades the electro-optical (E-O) properties of samples due to the stronger anchoring effect of the polymer on LC molecules.[23,24] In addition, the hysteresis effect related to the incomplete recovery of actuated polymer networks is also a critical issue in such a polymer/liquid crystal system and the relevant applications. In order to resolve or mitigate the aforementioned problems, several methods[25,26] have recently been successfully proposed. Wang *et al.* reduced the driving voltage and hysteresis by doping a small amount of ferroelectric nanoparticles into the system. Correspondingly, the Kerr constant was significantly increased simultaneously.[27] The coupling effect of polymer stabilization and the nanoparticle suspension has been found to play an important role. Su *et al.* enhanced the conductivity of the polymer networks by adding polyaniline functionalized graphene, and its effects on the performance of PSBPLC were investigated.[28] Yang *et al.* synthesized a judiciously designed polymerizable bent-shaped monomer to achieve a stable BPLC in virtue of the double effect of this kind of material. The BP was stabilized owing to the bent-shaped geometry of the monomer and further enhanced by a following polymerization.[29] The sample showed almost hysteresis-free operation accompanied by ultra-fast responsiveness. However, the driving voltage remained relatively high. To date, although polymer stabilization has been improved from the materials and methodologies, the required polymer concentration to achieve BP stabilization is still much higher, and thereby the aforementioned problems could only be balanced to some extent.

In general, H-bonds consist of the hydrogen atom of a hydroxyl or carboxyl group (H-bond donor) and a strongly electronegative nitrogen, oxygen or fluorine atom (H-bond acceptor), which contains a lone pair of electrons.[30,31] The intensity of H-bonds is between that of van der Waals forces and covalent bonds, and could serve as the force to assemble soft functional molecules into supramolecular structures.[32,33] In addition, they could self-assemble to stable complexes with molecular conformation in resemblance with typical LC molecules.[34,35] Thus, H-bonds are potentially desired in LC research and have already attracted both fundamental science and engineering interests. He *et al.* introduced chirality into the BPLC system through a chiral donor linked with an achiral acceptor *via* the H-bond. This creative molecular design enabled the BP operation range to be widened to 23 °C.[36] The LC host linked by a weak H-bond may be more easily twisted by additional charity dopants compared to those linked by covalent bonds, and tends to stabilize towards a double twist superstructure which is beneficial for BP stabilization.[37,38]

Herein, we propose a judiciously designed material to effectively reduce the concentration of polymer (*i.e.*, monomer concentration of the pre-polymerized mixture) which is necessarily higher in the conventional PSBPLC system, while still keeping a satisfactory structural stability as well as improved E-O properties by functionalizing the polymer/liquid crystal system with an H-bond complex. The polymerizable H-bond acceptor molecule, 4-vinyl pyridine (4VP), crosslinks with an LC-like two-functionality acrylate-based monomer denoted as RM257, forming an H-bond acceptor decorated polymer network. On the other hand, mesogenic cyano-biphenyl hydroxyl (CBH), with a chemical structure similar to that of conventional LC molecules, is selected as the donor molecule and is mixed with an LC host to prepare an LC donor. The results indicate that a stable and well-defined BPII simple cubic superstructure with a low driving voltage and weak hysteresis, forming in the polymer/LC system containing only 5.4 wt% polymer which is almost a half compared to the conventional PSBPLC system, is achieved by H-bond complex functionalization. Such an effective and efficient method, which could stabilize soft cubic BP structures by the combination effects of polymer anchoring and an auxiliary enhancement of H-bonds, has not been developed so far. The material system developed herein may be a competitor to the conventional BPLC material, thus providing a new selection and sweeping the current obstacles for the potential applications on high-speed image and information processing and others beyond.

2. Experiments

2.1. Materials

As schematically illustrated in Fig. 1(a), BPLC was prepared by homogeneously mixing the commercial nematic LC, TEB300 (provided by Slichem Co., Ltd, China, Δn = 0.166 (589 nm, 20 °C), $\Delta\varepsilon$ = 29.3 (1 kHz, 20 °C), T_{N-I} = 63 °C), and the conventional chiral agent, R5011 (supported by HCCH, China). To generate an H-bond complex functionalized system, herein, CBH (provided by Adams Reagent Co., Ltd) and 4VP (provided by Meryer Co., Ltd)

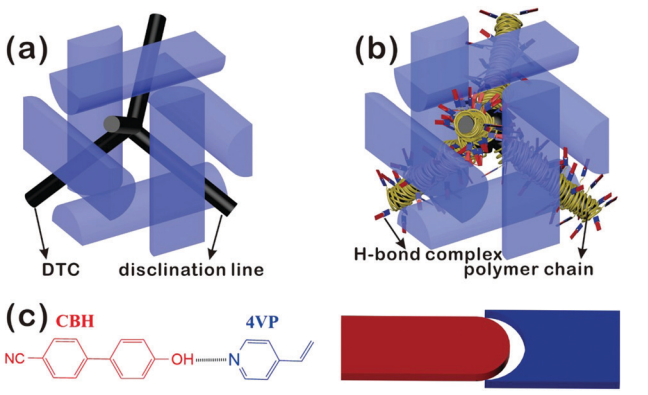

Fig. 1 (a) A schematic diagram of unit BPII lattices with disclination lines. The black rods represent the defect core and the blue columns represent the double twist cylinders. (b) The BP cubic polymer/liquid crystal system functionalized by H-bond complexes. The yellow lines surrounding the defect core represent the polymer network functionalized by the H-bond complex. (c) The chemical structure of the precursor: the left red part represents the donor CBH and the right blue part represents the acceptor 4VP, which was decorated on the polymer network through photo-polymerization.

Table 1 The chemical components and BP temperature ranges of the samples before and after UV exposure, as determined by POM at a cooling rate of 0.3 °C min^{-1}

	Component/wt%						BPLC temperature range/°C	
Sample	RM257	4VP	CBH	IRG184	TEB300	R5011	Before exposure UV	After exposure UV
A	6	3	0	0.4	87.1	3.5	50–54.1	−40[a] to 55
B1	3.6	1.8	3.34	0.4	87.76	3.5	50.5–53.5	−40[a] to 55.3
B2	3.6	1.8	0	0.4	90.7	3.5	50.5–54.5	48.2–55.3
C1	3.2	1.6	2.97	0.4	88.33	3.5	54.5–58	48.3–57.1
C2	3	1.8	3.34	0.4	87.96	3.5	51–55	40.5–57

[a] −40 °C is the lowest temperature point the hot-stage can reach.

(Fig. 1(c)) were cautiously selected as the proton donor and acceptor, respectively. CBH has a positively charged hydrogen atom, whose peripheral electron is withdrawn by the strong electronegativity of the oxygen atom, while 4VP has a negatively charged nitrogen atom, therefore generating a H-bond complex as shown in Fig. 1(c). It is noteworthy that 4VP is a polymerizable monomer with a single double bond and could form polymer networks under the assistance of the LC-like acrylate-based monomer RM257 with the functionality of two polymerizable acrylate groups. Moreover, the donor CBH has a similar molecular structure as the traditional LC molecules, thereby avoiding the adverse effects of incompatibility on the E-O properties of the sample.[39] In addition, a small amount of photo-initiator, Irgacure 184 (supported by BASF), is necessary for carrying out polymer stabilization with the irradiation of ultra violet (UV) light. Table 1 shows the compositions of pre-polymerized samples containing different contents of monomers and H-bond complex, while the molar ratio between 4VP and CBH is maintained at 1 : 1 to ensure maximized complexation of the acceptors and donors.

2.2. Sample testing

The mixtures were homogeneously stirred at isotropic phase, *i.e.*, 58 °C, for at least 1 h and injected into a 5 μm-thick LC cell assembled with two glass substrates without any surface treatment. The phase transition behaviour of the mixtures was investigated using a polarizing optical microscope (POM, Eclipse LV100POL, Nikon) with crossed polarizers under reflection mode and the optical textures were captured by a charge-coupled device (CCD, DS-U3). The reflection spectra of the sample were monitored by a fibre spectrometer (ULS2048, Avantes) connected to the POM. A precisely-controlled hot-stage (LTS120E, Linkam, controlled temperature range: −40–120 °C) was fixed on the POM to cool the sample from the isotropic state to the BPII state at a rate of 0.3 °C min^{-1}, followed by light irradiation with a UV source (365 nm, 3.1 mW cm^{-2}) for about 25 min to implement polymer stabilization of the BPII cubic structure. The Kössel diagram was detected by a microscopic imaging system in the reflection mode using a monochromatic laser source and a high numerical aperture (NA) oil immersed objective (×100, NA 1.25, Nikon), and the corresponding diagram was received at the back focal plane of the objective. The E-O performances were studied by confining the sample in a 12 μm-thick cell with the interdigitated stripe-shaped electrodes on a single substrate (width of the electrodes: 15 μm; gap between adjacent electrodes: 15 μm). A 1 kHz alternating current (AC) electric-field was applied to the cell to drive the BPLC; while a linear polarized He–Ne laser with a wavelength of about 633 nm was used as the probe beam and impinged along the cell normal. The polarization direction of the probe beam was at 45° with respect to the stripe-shaped electrodes to achieve the largest transmission contrast between the OFF (*i.e.*, absence of voltage) and ON (*i.e.*, applying a saturation voltage) states. The response time was detected using a photoelectric converter connected to an oscilloscope, and the Kerr constant of the sample was determined by fitting the electric-field dependent birefringence curve according to the extended Kerr theory.[40]

3. Result and discussion

Distinct from the common methods reported previously, in which the H-bond acceptors or donors existing in the pre-polymerized mixture were not polymerizable, herein the commonly used acrylate monomer, such as 2-ethylhexyl acrylate, was replaced by a cautiously considered polymerizable H-bond acceptor, 4VP, to modulate the crosslinking density of the polymer network on one hand as well as enhance the arrangement of the BP cube on the other hand. When the monomer concentration, including the commonly used LC-like monomer RM257 and H-bond acceptor 4VP, reached 5.4 wt%, and a proper amount of H-bond donor CBH with an equal molar content with 4VP was doped homogeneously in the system (*i.e.*, sample B1), the mixture showed a typical colourful platelets texture of BP during precisely controlled cooling from 53.5 °C to 50.5 °C, displaying a blue-shift of the corresponding reflection spectrum in the temperature range between 53.5 °C and 51.5 °C, while a red-shift during a further cooling to 50.5 °C (Fig. 2(a)). The sample was maintained at 51.7 °C for at least 1 h to avoid the possible hydrodynamic instability of the BP arrangement, followed by photo-polymerization. The treated sample presented a surprising BP range from 55.3 °C to lower than −40 °C (Fig. 2(b)), however the texture of the BP at lower than −40 °C was not determined due to the limitation of the hot stage. Furthermore, the corresponding Kössel diagram exhibited an almost unchanged circular ring in the whole BP range (Fig. 2(c)), which was similar to that observed before photo-polymerization (inset of Fig. 2(a)), thereby confirming a satisfying effect of structural enhancement of the BP cube with such a concentration. Nevertheless, a similar stable BP was not achieved in the system with the same content of polymer but without H-bond functionalization, *i.e.*, sample B2, until the content of polymer was gradually increased to 9.0 wt%, *i.e.*, sample A (Fig. S1, ESI†). By combining

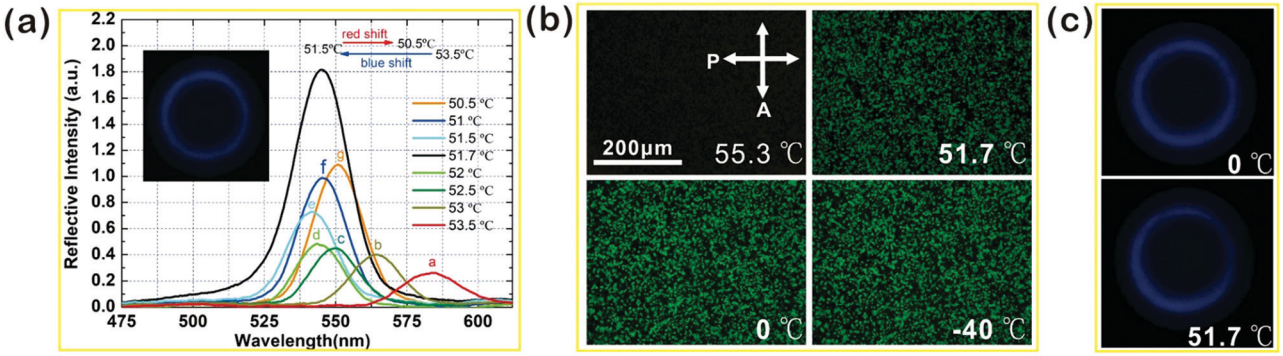

Fig. 2 (a) The reflection spectra of sample B1 at different temperatures during the cooling process. The inset is the corresponding Kössel diagram at a temperature of 51.7 °C. (b) The texture of sample B1 after UV exposure during cooling. BP texture is hardly seen at 55.3 °C, however the textures at 51.7 °C, 0 °C and even −40 °C are almost identical, which indicates a satisfying structural stabilization. Scale bar: 200 μm. (c) The Kössel diagram of the stabilized sample is almost unchanged during the cooling process, and is identical to that before the stabilization treatment.

the reflection spectra and Kössel diagrams, it is noteworthy that a stable BPII cubic superstructure with a much wider temperature range covering the whole room temperature range down to extremely low environmental temperatures can be obtained, which is still challenging to date.

The results of infrared spectrometry further corroborated the generation of H-bonds between the pyridines grafted on the polymer network and the biphenyl hydroxyls of the CBH molecules (Fig. 3). The 4VP molecules have a characteristic peak at 993 cm^{-1} corresponding to the pure pyridine ring absorption, while the CBH have no absorption at such a wavenumber. With the addition of CBH, it can be observed that the original peak at 993 cm^{-1} shifted to 997 cm^{-1} and finally to 1003 cm^{-1} which resulted from the formation of H-bonds between the pyridine ring and biphenyl hydroxyls of CBH.[41] On the other aspect, prior work reported that BP can be induced by an H-bond complex without molecular chirality owing to the promotion of intermolecular twist.[42]

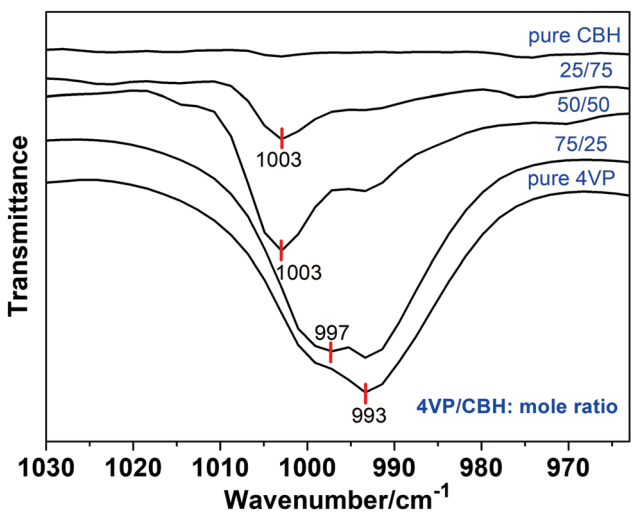

Fig. 3 The infrared spectra of the sample with different mole ratios of H-bond acceptor and donor. By increasing the proportion of the CBH, the peak shifts from 993 cm^{-1} to 1003 cm^{-1} due to the formation of H-bonds between the pyridine group and the biphenyl hydroxyls.

We predicted that a similar effect might exist in the system proposed herein. Thus, a nematic LC containing an appropriate amount of H-bond complexes (*i.e.*, nematic LC host: 94.29 wt%, 4VP: 2.00 wt%, CBH: 3.71 wt%) was specifically designed to confirm and clarify the prediction. The mixture was injected into a planar alignment treated Cano wedge LC cell at the clearing point by capillarity and cooled slowly. Simultaneously, the corresponding optical texture presented a series of straight dark disclination lines which is the typical optical texture of N* phase in a wedge cell. This texture was almost invariable during the whole cooling process (Fig. 4). The helical twisting power (HTP) induced from the H-bond complexes was calculated to be 0.48 μm^{-1} through the space of the adjacent disclination lines, R, and the angle between the two substrates, θ (Fig. S2, ESI†). It has been demonstrated previously that rising HTP plays a positive role in the stabilization of BPLCs.

Fig. S3 (ESI†) and Table 1 indicate that the BP range was extended by more than 80% by doping just a small amount of H-bond complexes, by comparing samples C1 to C2 (Fig. S3, ESI†).

The E-O performances of the H-bond complex functionalized BPLCs (*i.e.*, samples B1, C1 and C2) were investigated and compared with those of the conventional BPLCs without such functionalization (*i.e.*, samples A and B2), as shown in Table 2. It is noteworthy that a lower driving voltage and a weaker E-O hysteresis of H-bond functionalized sample B1 was achieved (Fig. 5). A lower polymer content of sample B1 led to a significant decrease in the driving voltage for about 30% compared to that of sample A. In addition, the BP state could be maintained, even when applied with a 100 V voltage (Fig. S4, ESI†); however the sub-millisecond response times of sample B1, both the rise and decay times, were still

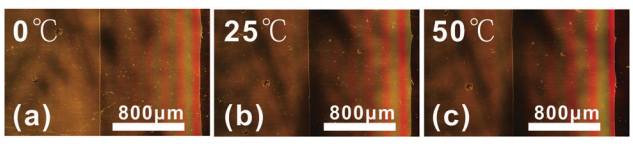

Fig. 4 POM micrographs of the nematic LC containing H-bond complexes injected into a Cano wedge cell. The straight disclination lines, which are a typical texture of N* phase confined in a wedge cell, seem to be invariable during the sample cooling.

Table 2 The E-O performances of samples A and B1 measured at 25 °C. Samples B2, C1 and C2 were measured at 50 °C due to the BPLC temperature range after polymerization

	Composition of the sample/wt%		LC and physical properties AFTER polymerization					
Sample	Total monomer amount[a]	Amount of the CBH[b]	BPLC temperature range/°C	Driving-voltage/V_{rms}	Hysteresis/%	Kerr constant/nm/V^2	Rise time/ms	Decay time/ms
A	9	0	−40 to 55	122	5.7	1.258	0.886	0.827
B1	5.4	3.34	−40 to 55.3	85	2	2.172	0.754	0.971
B2	5.4	0	48.2–55.3	118	6.2	1.065	0.732	0.992
C1	4.8	2.97	48.3–57.1	108	3.5	1.314	0.727	1.024
C2	4.8	3.34	40.5–57	101	3.1	1.396	0.716	1.132

[a] The monomer comprises RM257 and 4VP. [b] More H-bond donor CBH amount means stronger H-bond intensity.

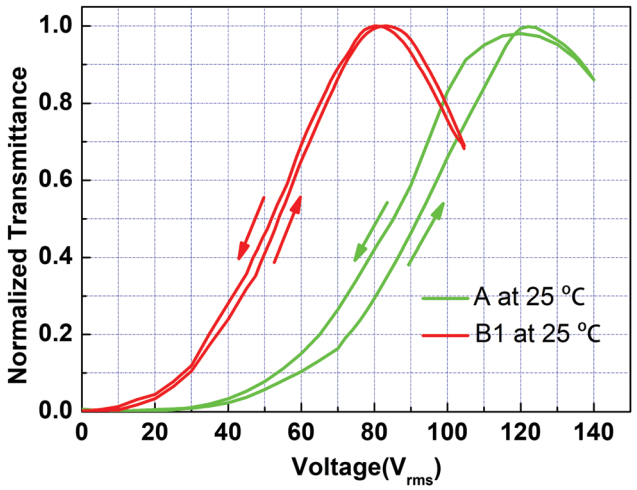

Fig. 5 Voltage-dependent-transmittance (*V*–*T*) curves of the H-bond functionalized sample B1 containing 5.4 wt% polymer and the conventional PSBPLC sample A containing 9 wt% polymer.

maintained, rather than prolonged due to the looser polymer network. Therefore the corresponding Kerr constant of sample B1 was predicted to be almost twice that of sample A. A weak E-O hysteresis is preferable in the polymer/LC system and is shown to be desirable for both photonic, and other perspective, applications. Nevertheless, the system with a higher polymer concentration is generally accompanied by a weaker E-O hysteresis.[43] Herein, a dramatic weakening of hysteresis with respect to the sample B1 (*i.e.*, 2%) was found surprisingly, though its polymer concentration is significantly lower than that of sample A (*i.e.*, 9%). Such a fantastic phenomenon might be ascribed to the molecular interaction between the H-bond acceptor (CBH) and the donor (4VP) grafted polymer, which means that the CBH molecules, which are out of equilibrium in a driven state, are quickly pulled back to their equilibrium position due to the H-bond interaction when the driving voltage is removed, thereby restraining E-O hysteresis. In addition, the E-O performances of the H-bond functionalized sample B1 still maintained a weak E-O hysteresis, even at temperatures as low as −15 °C (Fig. S5, ESI†), however the response time rose to the millisecond scale due to the decrease of molecular dynamic activation energy at such a low temperature, therefore providing a reference aiming towards the possible applications of BPLC in a low-temperature environment.

4. Conclusions

In conclusion, a stable BPII soft cubic superstructure with a temperature range from 55.3 °C to lower than −40 °C, enabled by an H-bond complex functionalized polymer/LC system, was achieved. The H-bond, generated from the complexation between the mesogenic proton acceptor (CBH) and the polymerizable proton donor (4VP) grafted on polymer network, not only enhanced the stability of the BP cubic superstructure, but promoted the intermolecular twist which played a positive role to achieve a stable BP cube. A significant advantage of such a material system is that the polymer concentration, which is necessarily high in common PSBPLCs, can be declined, and the E-O performances of BPLC are thus improved. Results indicate that a stable BPLC is achieved when the polymer concentration reaches 5.4 wt%, which is only 60% of that of common PSBPLC, thereby leading to a reduction in the driving voltage of more than 30%. The response time can be maintained at a sub-millisecond scale, rather than be prolonged by the lower polymer content. It is noteworthy that a conspicuous weakening of the E-O hysteresis of the BPLC (*i.e.*, 2%), commonly existing in a system with high polymer content, is exhibited in the H-bond complex functionalized system, which is probably caused by the H-bond interaction between the mesogenic acceptor, the CBH and the 4VP donor grafted on the polymer network. This proposed material offers distinct insight into BP stabilization and is promising as a strong candidate or competitor for conventional BP materials.

Conflicts of interest

There are no conflicts to declare.

Acknowledgements

We are grateful for the financial support of the Natural Science Foundation of China (Grant No. 61822504, 51873060, 61575063, 21574039, 61505131 and 61435008), the Shanghai Rising-Star Program (No. 17QA1401100), and the State Key Laboratory of Applied Optics (No. M200-D-1716).

Notes and references

1 V. Sharma, M. Crne, J. O. Park and M. Srinivasarao, *Science*, 2009, **325**, 449–451.

2 A. H. Groeschel, A. Walther, T. I. Loebling, F. H. Schacher, H. Schmalz and A. H. E. Mueller, *Nature*, 2013, **503**, 247–251.
3 S. S. Gandhi and L. C. Chien, *Adv. Mater.*, 2017, **29**, 1704296.
4 H. Kikuchi, *Struct. Bonding*, 2008, **128**, 99.
5 A. Yoshizawa, *RSC Adv.*, 2013, **3**, 25475–25497.
6 S. Yokoyama, S. Mashiko, H. Kikuchi, K. Uchida and T. Nagamura, *Adv. Mater.*, 2006, **18**, 48–51.
7 C. W. Chen, C. C. Li, H. C. Jau, L. C. Yu, C. L. Hong, D. Y. Guo, C. T. Wang and T. H. Lin, *ACS Photonics*, 2015, **2**, 1524–1531.
8 M. Wang, C. Zou, J. Sun and H. Yang, *Adv. Funct. Mater.*, 2017, **27**, 1702261.
9 W. F. Brinkman and P. E. Cladis, *Phys. Today*, 1982, **35**, 48–54.
10 S. Meiboom, J. P. Sethna, P. W. Anderson and W. F. Brinkman, *Phys. Rev. Lett.*, 1981, **46**, 1216–1219.
11 I. Dierking, W. Blenkhorn, E. Credland, W. Drake, R. Kociuruba, B. Kayser and T. Michael, *Soft Matter*, 2012, **8**, 4355–4362.
12 M. D. A. Rahman, S. M. Said and S. Balamurugan, *Sci. Technol. Adv. Mater.*, 2015, **16**, 033501.
13 E. Karatairi, B. Rozic, Z. Kutnjak, V. Tzitzios, G. Nounesis, G. Cordoyiannis, J. Thoen, C. Glorieux and S. Kralj, *Phys. Rev. E: Stat., Nonlinear, Soft Matter Phys.*, 2010, **81**, 041703.
14 L. Wang, W. He, X. Xiao, F. Meng, Y. Zhang, P. Yang, L. Wang, J. Xiao, H. Yang and Y. Lu, *Small*, 2012, **8**, 2189–2193.
15 Z. G. Zheng, D. Shen and P. Huang, *New J. Phys.*, 2010, **12**, 113018.
16 L. Wang, W. He, X. Xiao, Q. Yang, B. Li, P. Yang and H. Yang, *J. Mater. Chem.*, 2012, **22**, 2383–2386.
17 H. Kikuchi, M. Yokota, Y. Hisakado, H. Yang and T. Kajiyama, *Nat. Mater.*, 2002, **1**, 64–68.
18 Y. Hisakado, H. Kikuchi, T. Nagamura and T. Kajiyama, *Adv. Mater.*, 2005, **17**, 96–98.
19 Y. Li, S. Huang, P. Zhou, S. Liu, J. Lu, X. Li and Y. Su, *Adv. Mater. Technol.*, 2016, **1**, 1600102.
20 Y. Chen, J. Yan, J. Sun, S. T. Wu, X. Liang, S. H. Liu, P. J. Hsieh, K. L. Cheng and J. W. Shiu, *Appl. Phys. Lett.*, 2011, **99**, 201105.
21 O. Thet Naing, T. Mizunuma, Y. Nagano, H. Ma, Y. Ogawa, Y. Haseba, H. Higuchi, Y. Okumura and H. Kikuchi, *Opt. Mater. Express*, 2011, **1**, 1502–1510.
22 J. Yan and S. T. Wu, *J. Disp. Technol.*, 2011, **7**, 490–493.
23 Y. Chen and S. T. Wu, *J. Appl. Polym. Sci.*, 2014, **131**, 596–602.
24 M. S. Kim and L. L. Chien, *Soft Matter*, 2015, **11**, 8013–8018.
25 J. L. Zhu, S. B. Ni, Y. Song, E.-W. Zhong, Y. J. Wang, C. P. Chen, Z. Ye, G. He, D. Q. Wu, X. L. Song, J. G. Lu and Y. Su, *Appl. Phys. Lett.*, 2013, **102**, 071104.
26 Y. Chen, D. Xu, S. T. Wu, S.-I. Yamamoto and Y. Haseba, *Appl. Phys. Lett.*, 2013, **102**, 141116.
27 L. Wang, W. He, Q. Wang, M. Yu, X. Xiao, Y. Zhang, M. Ellahi, D. Zhao, H. Yang and L. Guo, *J. Mater. Chem. C*, 2013, **1**, 6526–6531.
28 S. Ni, H. Li, S. Li, J. Zhu, J. Tan, X. Sun, C. P. Chen, G. He, D. Wu, K.-C. Lee, C. C. Lo, A. Lien, J. Lu and Y. Su, *J. Mater. Chem. C*, 2014, **2**, 1730–1735.
29 W. Q. Yang, G. Q. Cai, Z. Liu, X. Q. Wang, W. Feng, Y. Y. Feng, D. Shen and Z. G. Zheng, *J. Mater. Chem. C*, 2017, **5**, 690–696.
30 I. Rozas, *Phys. Chem. Chem. Phys.*, 2007, **9**, 2782–2790.
31 U. Flierler, D. Stalke, A. Madsen and J. Overgaard, *Electron Density and Chemical Bonding I*, Springer, 2012, pp. 214–252.
32 S. J. Grabowski, *J. Phys. Org. Chem.*, 2004, **17**, 18–31.
33 S. D. Feyter, A. Miura, S. Yao, Z. Chen and F. Wurthner, *Nano Lett.*, 2005, **5**, 77–81.
34 W. L. He, H. Gu, P. Zhao, Z. Yang, H. Cao and D. Wang, *Liq. Cryst.*, 2017, **44**, 593–602.
35 C. C. Han, Y. C. Chou, S. Y. Chen and H. C. Lin, *RSC Adv.*, 2016, **6**, 32319–32327.
36 W. L. He, G. H. Pan, Z. Yang, D. Y. Zhao, G. G. Niu, W. Huang, X. T. Yuan, J. B. Guo, H. Cao and H. Yang, *Adv. Mater.*, 2009, **21**, 2050–2053.
37 Y. Shi, X. Wang, J. Wei, H. Yang and J. Guo, *Soft Matter*, 2013, **9**, 10186–10195.
38 W. L. He, L. Wang, Z. Yang, H. Yang and M. W. Xie, *Liq. Cryst.*, 2011, **38**, 1217–1225.
39 R. Kizhakidathazhath, H. Higuchi, Y. Okumura and H. Kikuchi, *ChemistrySelect*, 2017, **2**, 6728–6731.
40 J. Yan, H.-C. Cheng, S. Gauza, Y. Li, M. Jiao, L. Rao and S. T. Wu, *Appl. Phys. Lett.*, 2010, **96**, 071105.
41 S. W. Kuo, C. L. Lin and F. C. Chang, *Polymer*, 2002, **43**, 3943–3949.
42 Y. Li, Y. Cong, H. Chu and B. Zhang, *J. Mater. Chem. C*, 2014, **2**, 1783–1790.
43 Y. F. Lan, C. Y. Tsai, J. K. Lu and N. Sugiura, *Polymer*, 2013, **54**, 1876–1879.